

mutants display an osmotic avoidance defective (Osm) phenotype that is rescued by introduction of a DYF-18::GFP translational fusion construct. Wild type serves as a positive control, *osm-5* mutants serve as a negative control. (C, D) n denotes the number of animals tested. (*) Student's t-tests were performed for statistical significance (p values are shown). (E, F) Expression pattern and localization of the DYF-18 protein in head and tail neurons, respectively. A DYF-18::GFP translational fusion construct is expressed in amphid, phasmid and labial neurons in wild-type animals. The encoded protein localizes diffusely within the cell bodies, dendrites, and ciliary compartments. Cell bodies, dendrites and ciliary regions are indicated.

Figure 4 – DYF-18 regulates the localization of intraflagellar transport (IFT) machinery components. Both amphid and phasmid cilia are shown. (A, B) Localization of IFT subcomplex B proteins. CHE-2 shows wild-type localization whereas OSM-5 is largely excluded from cilia and accumulates at the base of cilia. (C, D) Localization of IFT motors. KAP-1 shows essentially wild-type localization with occasional accumulations at the tip of the middle segment (marked by *) whereas the OSM-3 motor is largely unable to enter the distal segment and shows large accumulations (marked by *) between the middle and the distal segment. (E) Shows the essentially normal localization of the IFT subcomplex A protein CHE-11 to the middle and distal ciliary segments. In all panels the dotted line divides the middle and the distal segments. BB, degenerate basal bodies; *, marks protein accumulation. Presence or absence of IFT in the mutant has been denoted.

Supplemental Table 1 – List of *C. elegans* strains and transgenes used in this study.

Supplemental Table 2 – List of genes with a 1.5 fold or greater change in expression levels in microarray analyses revealed to be statistically significant using both Class Comparison

and Significance Analysis for Microarrays (SAM) tools. Both tools identified a total of 1013 and 258 probe sets, respectively, given the above-mentioned criteria. These probe sets map to 881 genes in Class Comparison and 236 genes in SAM.

Supplemental Table 3 – Statistics and enrichment data for the gene classes depicted in Supplemental Figure 2 (as compared to the whole *C. elegans* genome).

Supplemental Figure 1 – A representative embryo staging experiment: conditions used for microarray and real-time PCR analyses are shown. Embryos at very early developmental stages obtained by alkaline bleach treatment were incubated in S-basal medium for 8 hours at 20°C. Worms at the L1 larval stage were subsequently removed by a second alkaline bleach treatment.

Supplemental Figure 2 – Distribution and enrichment diagrams for both gene ontology and protein domain representation for all statistically significantly downregulated genes identified using both the Class Comparison and SAM tools. Statistics and enrichment data for the depicted gene classes (as compared to the whole *C. elegans* genome) are shown in Supplemental Table 3.

Supplemental Figure 3 – DYF-17 does not affect the localization of ciliary proteins at the ciliary base and along the ciliary axoneme. The localization of the G protein-coupled receptor SRG-2 is unaffected in ASK cilia (A, D). The localization of the IFT motor OSM-3 is unaffected in amphids (B, E) and phasmids (C, F). Wild-type cilia (A-C) are full-length. As a result of the *dyf-17* mutation cilia are shortened (D-F). A schematic diagram depicting single amphid (head, left) and phasmid (tail, right) CSNs is shown in (G). In panels A-F, the scale bars measure 2 µm. *, demarcates the ciliary base.

Supplemental Figure 1

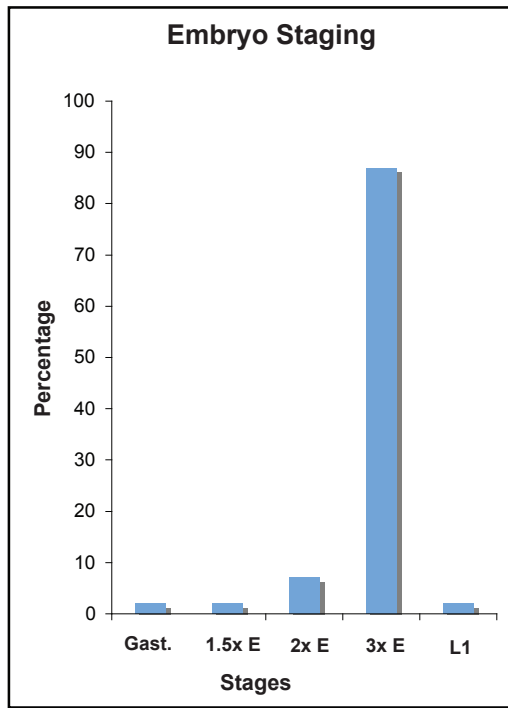
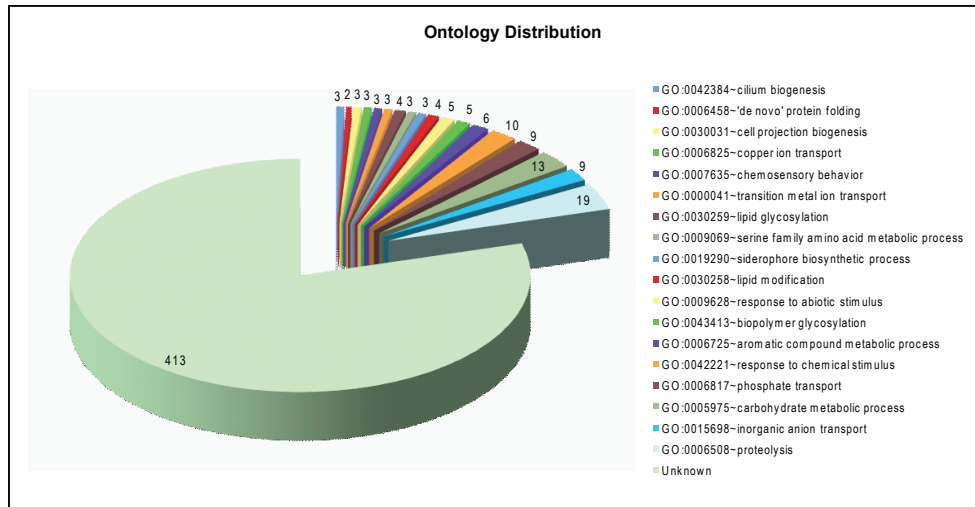


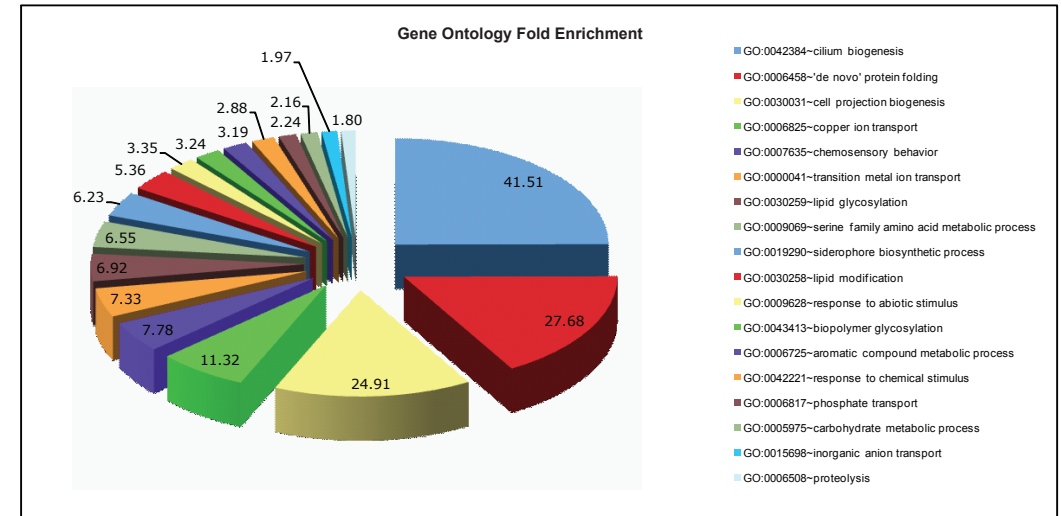
Figure Legend (X - axis)

- Gast. - Upto gastrulation stage embryos
- 1.5x E - Comma and 1.5-fold stage embryos
- 2x E - 2-fold stage embryos
- 3x E - 3-fold stage embryos
- L1 - L1 larvae

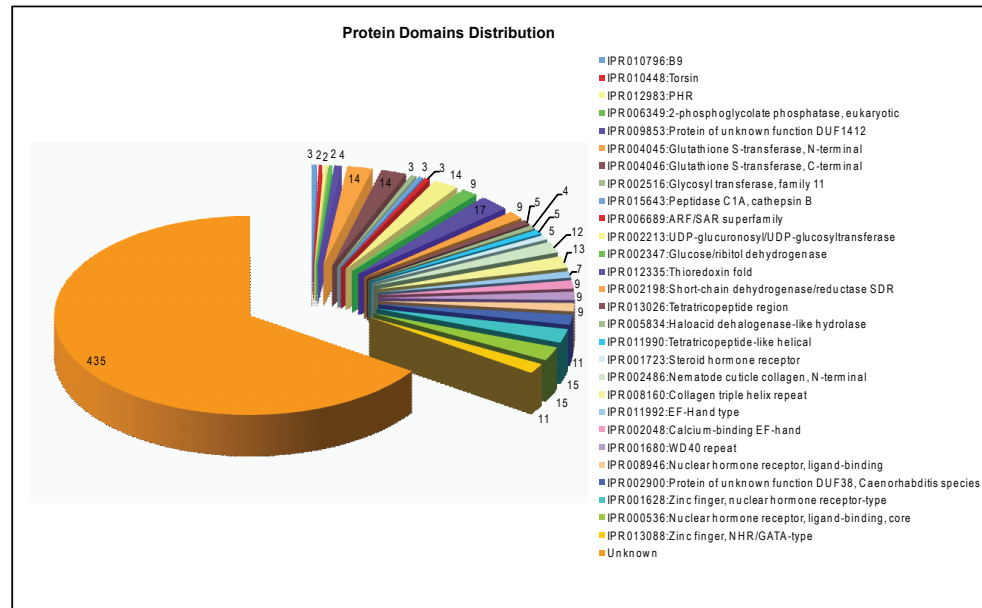
Supplemental Figure 2



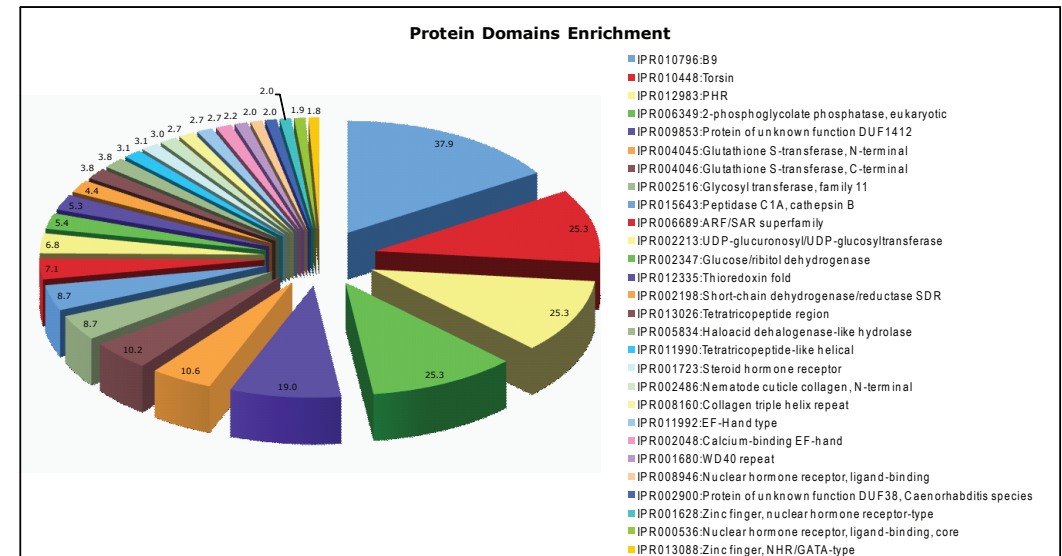
Supplemental Figure 2a: Gene Ontology distribution among the downregulated genes using Class Comparison.



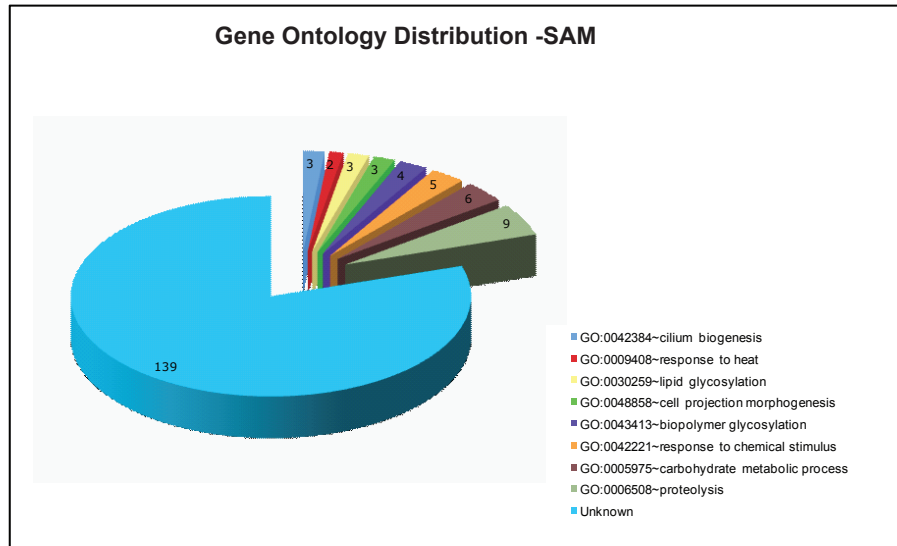
Supplemental Figure 2b: Gene Ontology enrichment among the downregulated genes using Class Comparison.



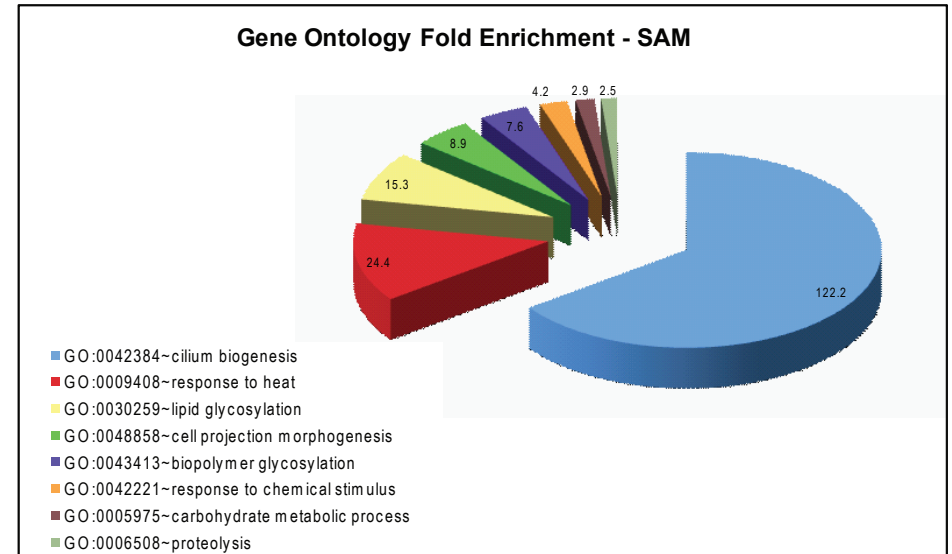
Supplemental Figure 2c: Protein domains distribution among the downregulated genes using Class Comparison.



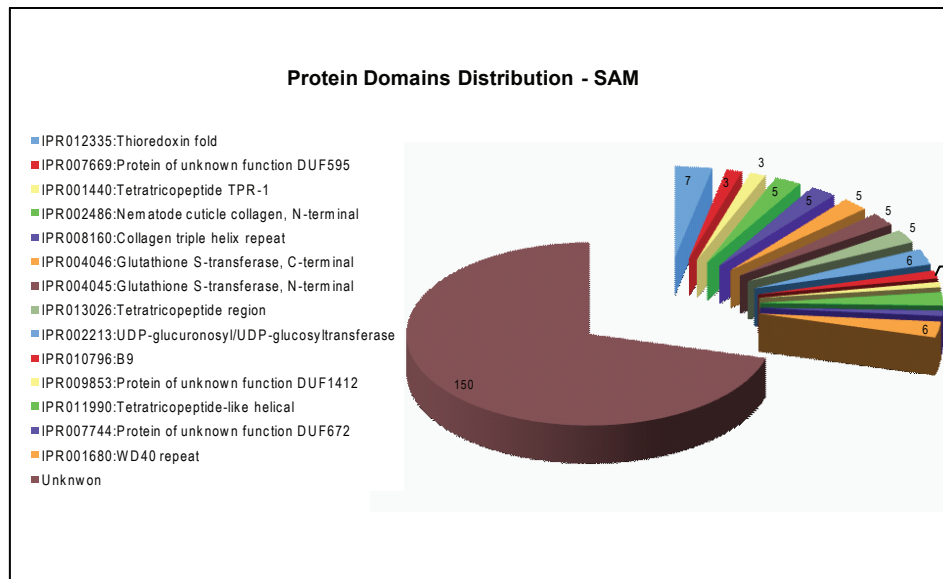
Supplemental Figure 2d: Protein domains enrichment among the downregulated genes using Class Comparison.



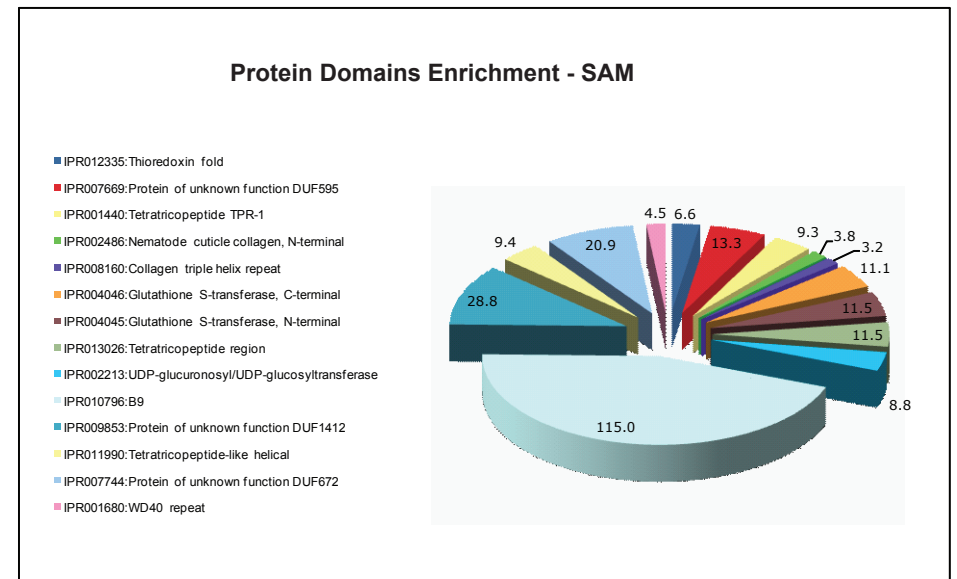
Supplemental Figure 2e: Gene Ontology distribution among the downregulated genes using SAM.



Supplemental Figure 2f: Gene Ontology enrichment among the downregulated genes using SAM.



Supplemental Figure 2g: Protein domains distribution among the downregulated genes using SAM.



Supplemental Figure 2h: Protein domains enrichment among the downregulated genes using SAM.

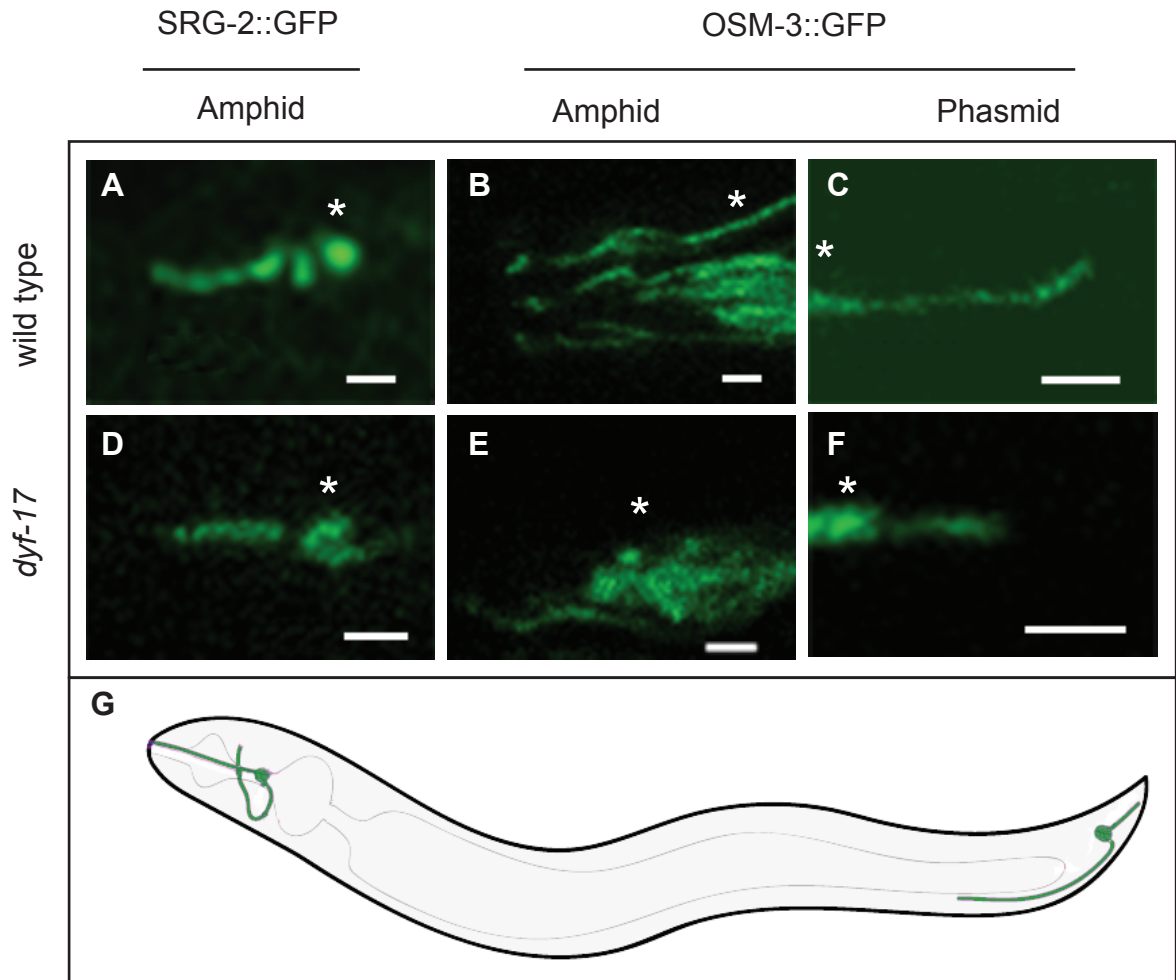


Table S1 – *C. elegans* strains and transgenes used in this study.

A. Strains

Strain	Genotype
CB3323	<i>che-13(e1805) I</i>
CX3344	<i>lin-15(n765ts) kyls53 X</i>
EG175	<i>dyf-17(ox175) V</i>
ET100	<i>dyf-18(ok200) IV</i> (6x outcrossed)
JT204	<i>daf-12(sa204) X</i>
JT5010	wild type N2 Bristol
JT6924	<i>daf-19(m86) II; daf-12(sa204) X</i>
MT3559	<i>dyf-9(n1513) V</i>
MX60	<i>myEx10</i>
MX254	<i>nxEx [kap-1]</i>
MX255	<i>ejEx1</i>
MX316	<i>nxEx [che-2]</i>
MX467	<i>dyf-18 IV; yhEx2</i>
MX468	<i>dyf-18 IV; nxEx [che-2]</i>
MX469	<i>dyf-18 IV; myEx10</i>
MX471	<i>dyf-18 IV; nxEx [kap-1]</i>
MX497	<i>dyf-18 IV; ejEx1</i>
OE3146	<i>daf-12(sa204) X; ofEx114</i>
OE3661	<i>dyf-17(ox175) V; ofEx461</i>
OE3663	<i>dyf-17(ox175) V</i> (2x outcrossed)
OE4013	<i>dyf-17(ox175) V</i> (4x outcrossed)
OE4101	<i>dyf-17(ox175) V; ofEx742</i>
OE4105	<i>dyf-17(ox175) V; ofEx746</i>
OE4106	<i>dyf-17(ox175) V; kyls141</i>
OE4107	<i>dyf-17(ox175) V; myls1</i>
OE4108	<i>dyf-17(ox175) V; kyls53</i>
OE4116	<i>ncl-1(e1865) unc-36(e251) III; osm-6(p811) V; mnls17; ofEx779</i>
OE4118	<i>dyf-17(ox175) V; kyEx123</i>
OE4119	<i>dyf-17(ox175) V; kyEx162</i>
PR813	<i>osm-5(p813) V</i>
SP2101	<i>ncl-1(e1865) unc-36(e251) III; osm-6(p811) V; mnls17</i>
YH2	<i>yhEx2</i>

B. Transgenes (extrachromosomal arrays and integrated transgenes)

Transgene	Genotype
<i>ejEx1</i>	<i>osm-3p::osm-3::gfp; rol-6(su1006)</i>
<i>kyEx123</i>	<i>tax-2p::tax-2::gfp; lin-15(+)</i>
<i>kyEx162</i>	<i>srg-2p::srg-2::gfp; lin-15(+)</i>
<i>kyls53</i>	<i>odr-10p::odr-10::gfp; lin-15(+)</i>
<i>kyls141</i>	<i>osm-9p::osm-9::gfp; lin-15(+)</i>
<i>mnls17</i>	<i>osm-6p::osm-6::gfp; unc-36(+)</i>
<i>myEx10</i>	<i>che-11p::che-11::gfp; rol-6(su1006)</i>
<i>myls1</i>	<i>pkd-2p::pkd-2::gfp; cc::GFP</i>
<i>nxEx</i>	<i>che-2p::che-2::gfp; rol-6(su1006)</i>
<i>nxEx</i>	<i>kap-1p::kap-1::gfp; rol-6(su1006)</i>
<i>ofEx114</i>	<i>bbs-7p::gfp; rol-6(su1006)</i>
<i>ofEx461</i>	<i>bbs-7p::gfp; elt-2p::mCherry</i>
<i>ofEx742</i>	<i>dyf-17p::dyf-17::gfp; che-13p::mCherry; elt-2p::mCherry</i>
<i>ofEx746</i>	<i>dyf-17p::dyf-17::gfp; elt-2p::mCherry</i>
<i>ofEx779</i>	<i>dyf-17p::dyf-17::mCherry; elt-2p::mCherry</i>
<i>yhEx2</i>	<i>osm-5p::osm-5::gfp; rol-6(su1006)</i>

Table S3 (Suppl)

Supplemental Table 3: Enrichment data for Supplemental Figure 2 (S2A+B)

Term	Count	P Value	Fold Enrichment
GO:0042384~cilium biogenesis	3	0.001689181	41.51
GO:0006458~'de novo' protein folding	2	0.070220875	27.68
GO:0030031~cell projection biogenesis	3	0.0054542	24.91
GO:0006825~copper ion transport	3	0.02728659	11.32
GO:0007635~chemosensory behavior	3	0.055063169	7.78
GO:0000041~transition metal ion transport	3	0.061444018	7.33
GO:0030259~lipid glycosylation	4	0.018972939	6.92
GO:0009069~serine family amino acid metabolic process	3	0.074903264	6.55
GO:0019290~siderophore biosynthetic process	3	0.081952367	6.23
GO:0030258~lipid modification	4	0.037308935	5.36
GO:0009628~response to abiotic stimulus	5	0.061006684	3.35
GO:0043413~biopolymer glycosylation	5	0.067016539	3.24
GO:0006725~aromatic compound metabolic process	6	0.038933819	3.19
GO:0042221~response to chemical stimulus	10	0.007699593	2.88
GO:0006817~phosphate transport	9	0.047515959	2.24
GO:0005975~carbohydrate metabolic process	13	0.017054217	2.16
GO:0015698~inorganic anion transport	9	0.086326258	1.97
GO:0006508~proteolysis	19	0.017776188	1.80
Unknown	413		